"Eventless" $InsP_3$-dependent SR-Ca^{2+} Release Affecting Atrial Ca^{2+} Sparks

Tamara Horn, Nina D. Ullrich & Marcel Egger

Department of Physiology
University of Bern
Bühlplatz 5
CH-3012 Bern, Switzerland

Running title: $InsP_3R$ Modulation of Calcium Sparks.

Keywords: $InsP_3$, Ca^{2+} Sparks, CICR, atrial myocytes

Total number of words: 4469 (excluding Figure Legends and References)

Address for correspondence:

Marcel Egger
Department of Physiology, University of Bern
Bühlplatz 5
CH-3012 Bern, Switzerland
Phone: fax: ++41 - 31 - 631 8737
E-mail: egger@pyl.unibe.ch

KEY POINT SUMMARY

- Inositol 1,4,5-trisphosphate receptors ($InsP_3Rs$) are functionally expressed in cardiac myocytes.
- Influence of inositol 1,4,5-trisphosphate-induced SR-Ca^{2+}release (IP3ICR) on atrial excitation-contraction coupling under physiological and pathophysiological conditions remains elusive.
- The present study focuses on local IP3ICR and its functional consequences for ryanodine receptor (RyR) activity and subsequent Ca^{2+}-induced Ca^{2+} release (CICR) in atrial myocytes.
- Here we show significant SR-Ca^{2+} flux but eventless SR-Ca^{2+} release through $InsP_3$ receptors.
- We suggest a new mechanism based on eventless and highly efficient $InsP_3$-dependent SR-Ca^{2+} flux as a crucial mechanism of functional crosstalk between $InsP_3Rs$ and RyRs, which may be an important factor in the modulation of excitation-contraction coupling sensitivity.

Word count: 121

ABSTRACT

Augmented inositol 1,4,5-trisphosphate receptor ($InsP_3R$) function has been linked to a variety of cardiac pathologies including cardiac arrhythmia. The contribution of inositol 1,4,5-trisphosphate-induced Ca^{2+} release (IP3ICR) in excitation-contraction coupling (ECC) under physiological conditions, as well as under cellular remodeling remain controversial. Here we test the hypothesis that local IP3ICR directly affects ryanodine receptor (RyR) function and subsequent Ca^{2+}-induced Ca^{2+} release (CICR) in atrial myocytes. IP3ICR was evoked by UV-flash photolysis of caged $InsP_3$ under whole-cell configuration of the voltage-clamp technique in atrial myocytes isolated from C57/BL6 mice. Photolytic release of $InsP_3$ was accompanied by a significant increase in the Ca^{2+} release event frequency (4.14±0.72 *vs*. 6.20±0.76 events*100$\mu m^{-1}s^{-1}$). These individual photolytically triggered Ca^{2+} release events were identified as Ca^{2+} sparks which originated from RyR openings. This was verified by Ca^{2+} spark analysis and pharmacological separation between RyR and $InsP_3R$-dependent SR-Ca^{2+} release (2-aminoethoxydiphenyl borate, xestospongin C, tetracaine). Significant SR-Ca^{2+} flux but eventless SR-Ca^{2+} release through $InsP_3R$ was characterized using SR-Ca^{2+} leak/SR-Ca^{2+} load measurements. These results strongly support the idea that IP3ICR can effectively modulate RyR openings and Ca^{2+} spark probability. We conclude that eventless and highly efficient $InsP_3$-dependent SR-Ca^{2+} flux is the main mechanism of functional crosstalk between $InsP_3Rs$ and RyRs, which may be an important factor in the modulation of ECC sensitivity.

ABBREVIATIONS

Inositol 1,4,5-trisphosphate-induced Ca^{2+} release	IP3ICR
Inositol 1,4,5-trisphosphate receptor	$InsP_3R$
Ca^{2+}-induced Ca^{2+} release	CICR
Excitation-contraction coupling	ECC
Ryanodine receptor	RyR
Sarcoplasmic reticulum	SR
Xestospongin	Xesto
Tetracaine	TET
2-Aminoethoxydiphenyl borate	2APB
Cyclopiazonic acid	CPA
Endothelin-1	ET-1

INTRODUCTION

In cardiac myocytes two mechanisms for SR-Ca^{2+} release have been established, Ca^{2+}-induced Ca^{2+} release (CICR) as the central mechanism for excitation-contraction coupling (ECC) and inositol 1,4,5-trisphosphate-induced Ca^{2+} release (IP3ICR), Ca^{2+} release *via* inositol 1,4,5-trisphosphate receptor ($InsP_3R$) activation. However, although $InsP_3Rs$ are functionally expressed in cardiac preparations (Mackenzie *et al*., 2004; Zima & Blatter, 2004; Domeier *et al*., 2008; Harzheim *et al*., 2009), their role under physiological as well as under pathophysiological conditions in ECC and CICR is still a matter of an ongoing debate.

It has been suggested that SR-Ca^{2+} release *via* $InsP_3R$ may effectively modulate ECC in ventricular cardiomyocytes, even though the expression of $InsP_3Rs$ is only a fraction of RyR expression levels (Lipp *et al*., 2000; Kockskämper *et al*., 2008). These aspects gain even more importance in atrial myocytes, where $InsP_3Rs$ are expressed 3-10 times more compared to ventricle myocytes (Lipp *et al*., 2000; Domeier *et al*., 2008). In addition, this hypothesis is supported by two key observations. First, under pathophysiological conditions, during cellular remodeling, $InsP_3R$ expression is upregulated and may cause delayed after depolarizations (DADs), which lead to arrhythmogenicity (Zima & Blatter, 2004; Bootman *et al*., 2007). Second, $InsP_3R$ deficient hearts are largely protected from pro-arrhythmogenic stress (Li *et al*., 2005). Supporting data that encourage a significant contribution of IP3ICR to ECC and CICR are colocalization studies of RyRs and $InsP_3Rs$ (Lipp *et al*., 2000; Mackenzie *et al*., 2002), the microarchitecture of atrial myocytes (Yamasaki *et al*., 1997) and functional studies that have been carried out (Mackenzie *et al*., 2002; Zima & Blatter, 2004; Li *et al*., 2005).

In atrial myocytes normal Ca^{2+} transient propagation by concentric Ca^{2+} waves, which are not pro-arrhythmogenic, may be facilitated by IP3ICR (Mackenzie *et al*., 2004). Local Ca^{2+} signaling between $InsP_3Rs$ / RyRs and *vice versa* might mediate a functional Ca^{2+} crosstalk between the two types of SR-Ca^{2+} release channels. This was conceptualized for smooth muscle cells, where local RyR Ca^{2+} release events, "Ca^{2+} sparks", were activated via CICR subsequent to $InsP_3R$ activation (Gordienko & Bolton, 2002).

In atrial cells, RyR is the major Ca^{2+} release channel, organized in clusters and functionally coupled (Niggli & Shirokova, 2007). On a local scale, RyR openings give rise to "Ca^{2+} sparks", the building blocks of global Ca^{2+} transients in cardiac cells (Cheng *et al*., 1993), while coordinated openings of clustered $InsP_3Rs$ will form "Ca^{2+} puffs" with distinct properties (Yao *et al*., 1995).

Along with microscopic Ca^{2+} release events (Ca^{2+} sparks and Ca^{2+} puffs) eventless Ca^{2+} release has been discovered ("Ca^{2+} quarks", "Ca^{2+} blips") (Parker *et al*., 1996; Lipp *et al*., 1996; Brochet *et al*., 2011). However, these largely invisible Ca^{2+} release events and concomitant Ca^{2+} fluxes may have a significant impact on Ca^{2+} signaling in sub-cellular microdomains and may be involved in the functional crosstalk between RyRs and $InsP_3$Rs, which is still enigmatic.

The present study focuses on local IP3ICR and its functional consequences for RyR activity in atrial myocytes. We examined local IP3ICR trigged by photoactivation of caged inositol 1,4,5-trisphosphate ($InsP_3$) in isolated atrial myocytes from mice under whole cell voltage-clamp conditions. This highly specific approach bypasses sarcolemmal membrane receptor activation and subsequent signaling cascades. Surprisingly, we found that although no individual IP3ICR events could be visualized, $InsP_3$ release significantly affected the Ca^{2+} spark probability and foster that RyR Ca^{2+} release can be modulated by Ca^{2+} release *via* $InsP_3$Rs in intracellular microdomains. This suggested a new mechanism based on highly efficient but "eventless" $InsP_3$-dependent SR-Ca^{2+} release. We conclude that invisible $InsP_3$-dependent SR-Ca^{2+} events are the main mechanism of functional crosstalk between $InsP_3$Rs and RyRs.

MATERIAL AND METHODS

Atrial myocytes from adult male C57/BL6 mice, obtained from the Central Animal Facility, University Hospital, University of Bern, were freshly isolated by Langendorff perfusion technique. Hearts were removed after animals were killed by cervical dislocation. The number of animals (N) and myocytes (n) are given in the figure legends. All experiments were performed at room temperature and approved by the State Veterinary Office of Bern, Switzerland, according to Swiss Federal Animal protection law. Whole-cell voltage clamp was combined with confocal Ca^{2+} imaging and UV-flash photolysis. The pipette solution contained (in mmol/L) 120 CsAsp, 10 HEPES, 20 TEA-Cl, 5 K-ATP, 1 $MgCl_2$, 0.1 K_5-fluo-3 (Biotium), 2 GSH, (0.03, 0.06, 0.24) caged $InsP_3$-6Na (Sichem); pH 7.2 with CsOH. Cells were perfused with external solution containing (in mmol/L) 140 NaCl, 5 HEPES, 1.1 $MgCl_2$, 5.4 KCl, 10 Glucose, 1.8 CaCl, 0.5 BaCl, 1 CsCl; pH 7.4 NaOH. Pharmacological experiments used 5 μM 2-aminoethoxydiphenyl borate (Fluka), 5 μM xestospongin C (A.G Scientific Inc.), 1 mM tetracaine (Sigma) or 10 mM caffeine (Sigma) added to the external solution. For Ca^{2+} leak/load experiments (Shannon *et al*., 2002) atrial myocytes were loaded with fluo-3 AM (Biotium).

Data are reported as mean ± SEM. Where the data was normally distributed, paired or unpaired, where appropriate, Student's t-test was applied. For not normally distributed data the Wilcoxon Matched-Pairs Signed-Ranks Test was applied. A detailed Materials and Methods section is available in the Online Data Supplement.

RESULTS

ET-1 induced $InsP_3R$ Ca^{2+} release in atrial myocytes

Figure 1 shows that rapid administration of 100 nM endothelin-1, an $InsP_3$ pathway activator, caused a significant increase in spontaneous local as well as global Ca^{2+} release events in resting mouse atrial cardiomyocytes. This increase was 2APB ($InsP_3R$ blocker) sensitive (Fig. 1B) and was also absent in control (Fig. 1C). Observations agreed with previously performed experiments from other groups (Mackenzie *et al*., 2004; Zima & Blatter, 2004; Li *et al*., 2005), that ET-1 mediated IP3RICR could be obtained in various mammalian species including mouse atrial myocytes. ET-1 triggered IP3ICR is based on a complex signaling cascade which involves G-protein coupled phospholipase C activation followed by diacylglycerol and $InsP_3$ production. To bypass this complex signal transduction pathway, $InsP_3Rs$ were activated by rapid and transient intracellular $InsP_3$ elevation induced by photorelease of $InsP_3$ from caged $InsP_3$.

$InsP_3$-induced Ca^{2+} release triggered by UV flash photolysis of caged $InsP_3$

Atrial myocytes were voltage-clamped in the whole-cell configuration of the patch-clamp technique and held at –80 mV. Caged $InsP_3$ in combination with the Ca^{2+} indicator fluo-3 were dialyzed into the cell through the patch pipette. A SR-Ca^{2+} loading protocol based on L-type Ca^{2+} current activation elicited by depolarization steps from -80 mV to 0 mV (up to 10 times) was applied to ensure comparable SR-Ca^{2+} content, before line scan images were recorded (Fig. 2A). Under these conditions spontaneous Ca^{2+} event activity of about 3.7±0.92 events*100$\mu m^{-1}s^{-1}$ was observed.

In order to evoke IP3ICR in a highly specific manner, global UV-flashes were applied to photorelease $InsP_3$ in the entire cytosol, which was followed by an increase of local Ca^{2+} event frequency triggered in a dose dependent manner (Fig. 2C). The number of Ca^{2+} release events observed after photorelease of $InsP_3$ was normalized to the number of spontaneous Ca^{2+} releases counted before $InsP_3$ uncaging. Caged $InsP_3$ concentrations of 30 μM and 60 μM caused a slight but not significant increase in the frequency of Ca^{2+} release events (30 μM: 2.73±0.51 to 3.06±0.71 events*100$\mu m^{-1}s^{-1}$; 60 μM: 4.03±0.73 to 4.20±0.58 events*100$\mu m^{-1}s^{-1}$). However, photolysis of 240

μM caged $InsP_3$ triggered a significant (p=0.02) increase in frequency of Ca^{2+} release events from 4.14±0.72 to 6.20±0.76 events*100$\mu m^{-1}s^{-1}$ (Fig. 2B and 2C). It is to be mentioned, that the effective $InsP_3$ concentration after UV-flash application is orders of magnitude lower but in proportion to the loading concentration of the caged compound in the pipette solution (see online data supplement). Figure 2C shows control experiments lacking the caged compound indicating that UV-flash application alone had no effect on the frequency of events. We expected, that at least part of the total number of photolytically triggered Ca^{2+} events were based on IP3ICR (e.g. Ca^{2+} "puffs"). Althought Ca^{2+} sparks shows similarities with Ca^{2+} puffs, it has been shown that Ca^{2+} puffs exhibit significantly distinct spatio-temporal properties, that are different from Ca^{2+} sparks (Cheng *et al*., 1993; Yao *et al*., 1995; Tovey *et al*., 2001; Niggli & Shirokova, 2007). At maximal event activity (240 μM caged $InsP_3$), local Ca^{2+} release events were analyzed in more detail for amplitude, full duration at half-maximum amplitude (FDHM), full width at half-maximum amplitude (FWHM), full duration (fulldur), full width (fullwidth) and rise time (Picht *et al*., 2007). Cells were divided into two groups: One group showed little (<1.3 events*100$\mu m^{-1}s^{-1}$) increase (frequency: 0.98±0.08 events*100$\mu m^{-1}s^{-1}$), a second group showed >1.3 events*100$\mu m^{-1}s^{-1}$ increase in Ca^{2+} release events (frequency: 3.24±0.55 events*100$\mu m^{-1}s^{-1}$) after photolytic $InsP_3R$ activation. Ca^{2+} release events obtained in both groups showed no significant difference in their temporal characteristics. The fullwidth was significantly larger in the group of cells that showed little increase in the frequency of Ca^{2+} release events, from 3.80±0.29 to 4.51±0.38 μm (Fig. 2D), an indication for contribution of IP3ICR in Ca^{2+} spark formation. Nevertheless, Ca^{2+} event analysis did not show the anticipated two classes of local Ca^{2+} release events (i.e. Ca^{2+} sparks and Ca^{2+} puffs). The obtained parameters of Ca^{2+} events were comparable to those reported for Ca^{2+} sparks (Niggli & Shirokova, 2007) and are summarized in the supplementary Table 1 in the online material.

However, control measurements revealed photolytically triggered local $InsP_3$ Ca^{2+} events (Ca^{2+} puffs) in neonatal rat cardiomyocytes. In other words, experimental conditions can be assumed to be appropriate for detecting microscopic subcellular Ca^{2+} events including Ca^{2+} puffs (see Fig. 2S, Supplementary Material).

While photorelease of $InsP_3$ lead to an increased Ca^{2+} spark frequency (Fig. 2), the precise mechanism by which this occurred still remained unclear. Therefore, pharmacological interventions were used to distinguish between Ca^{2+} sparks and Ca^{2+} puffs by selective inhibition of either RyRs or $InsP_3Rs$. To inhibit IP3ICR, cells were incubated for at least 20 min in 5 μM Xesto, or 5 μM 2APB was acutely applied. TET (1 mM) was applied to inhibit RyR Ca^{2+} release (Fig. 3A).

Photolytic increase of Ca^{2+} release events was inhibited by 2APB and Xesto, without affecting the spontaneous Ca^{2+} release event activity.

Surprisingly, in the presence of TET a complete inhibition of all Ca^{2+} release events (Fig. 3B and 3C) was observed. This observation is in full agreement with the Ca^{2+} event analysis given in Fig. 2, showing that all provoked SR-Ca^{2+} release events can be classified as Ca^{2+} sparks. Taken together, photolytically activated IP3ICR efficiently facilitates RyR Ca^{2+} release.

SR-Ca^{2+} load and invisible $InsP_3R$ Ca^{2+} release (SR-Ca^{2+} leak)

Ca^{2+} spark probability strongly depends on luminal Ca^{2+} ($[Ca^{2+}]_{SR}$). RyRs and $InsP_3Rs$ may share, at least in part, the same luminal Ca^{2+} pool, suggesting that $[Ca^{2+}]_{SR}$ may have a potential role in the functional crosstalk of both Ca^{2+} release channels, which was examined using caffeine induced Ca^{2+} transients. $InsP_3R$ block (Fig. 3D) did not significantly affect the SR-Ca^{2+} content (2APB: 1±0.18 to 1.09±0.08 a.u., p=0.8; and Xesto: from 1.13±0.07 to 0.78±0.09 a.u., p= 0.07), whereas TET caused a significant increase in the SR-Ca^{2+} content from 1±0.07 to 1.4±0.1 a.u., p=0.02, presumably by suppressing Ca^{2+} leak (Shannon *et al*., 2002). Besides the SR-Ca^{2+} content, SR-Ca^{2+} leak is an important determinant for Ca^{2+} spark frequency. Indirect evidence that $InsP_3R$ stimulation may play a role in SR-Ca^{2+} leak came from the observation, that in the presence of TET subsequent $InsP_3$ release caused a slow but significant increase in background fluorescence, which was not seen in the presence of 2APB (Fig. 3E). This result suggests that "eventless" Ca^{2+} flux through the $InsP_3R$, which cannot be resolved as local Ca^{2+} release events, may be more pronounced in atrial cardiomyocytes than previously expected.

In Figure 4 we addressed the question whether $InsP_3Rs$ may contribute to the SR-Ca^{2+} leak and thus affect the Ca^{2+} spark appearance by performing a modified SR-Ca^{2+} leak protocol introduced by Shannon et al. (Shannon *et al*., 2002). Atrial myocytes were field stimulated for 45 seconds at 1 Hz, followed by a rapid solution switch from 1.8 mM extracellular Ca^{2+} concentration ($[Ca^{2+}]_o$) to a nominally $[Ca^{2+}]_o$ free and $[Na^+]_o$ free solution. After 10s 10 μM cyclopiazonic acid (CPA, a potent SERCA blocker) was added and finally, 30 s later, the SR-Ca^{2+} content was measured with rapid caffeine application (Fig. 4A). Atrial myocytes were divided into two groups. The control group was recorded under conditions given above, the second group was pre-incubated with 100 nM ET-1 for at least 120 s before CPA was applied (Fig. 4A). CPA causes an inhibition of the SERCA function. Hence, in combination with the blocked Na^+/Ca^{2+} exchanger (NCX) function, any Ca^{2+} leaking from the SR is trapped in the cytoplasm and mirrored by an increase in the cytosolic Ca^{2+} concentration $[Ca^{2+}]_i$. This increase was measured and defined as SR-Ca^{2+} leak.

When CPA was added in the presence of ET-1 there was a significant increase in SR-Ca^{2+} leak ($\Delta[Ca^{2+}]_i$) compared to the leak in control (0.16±0.03 to 0.38±0.09 $\Delta F/F_0$, p=0.02). The SR-Ca^{2+} leak/SR-Ca^{2+} load relationship increased accordingly, although not significantly ($\Delta[Ca^{2+}]_i$/SR-Ca^{2+} load: 0.047±0.007 to 0.086±0.020, p=0.09). This may be due to the additional Ca^{2+} influx induced by ET-1 (He *et al*., 2000) causing an increased SR-Ca^{2+} content (3.30±0.24 to 4.53±0.26 F/F_0, p= 0.001). However, reduced SERCA activity unmasked a substantial contribution of $InsP_3R$ activity to the total SR-Ca^{2+} leak (Fig. 4) which was not seen before. Taken together, eventless $InsP_3R$-Ca^{2+} release flux is part of a Ca^{2+} leak and facilitates SR-Ca^{2+} spark probability.

DISCUSSION

The physiological role of atrial myocytes is to ensure ventricular blood refilling especially under conditions of physical stress and activity. This involves stimulation by direct autonomic nervous system innervation, neuro-humoral effects and interactions with hormones released by the vasculature which boost ECC on a cellular level. Similar to ventricular myocytes, the fundamental mechanism for ECC in atrial myocytes is driven by CICR. However, the contribution of IP3ICR in initiation, propagation and amplification of local and global SR-Ca^{2+} release and thus CICR in atrial myocytes remains controversial (Blatter *et al*., 2003; Mackenzie *et al*., 2004).

Our results obtained in atrial myocytes showed significant alterations in Ca^{2+} sparks (width and frequency) during $InsP_3R$ activation. This emphasizes that local Ca^{2+} release from $InsP_3Rs$ may play a significant role in the modulation of Ca^{2+}-dependent RyR activity in atrial myocytes. Our approach, based on the combination of different biophysical methods, revealed some discrepancies between $InsP_3R$ activation and the appearance of local SR-Ca^{2+} release events such as apparent invisible, "eventless" Ca^{2+} release although $InsP_3R$ activation occurred. From these discrepancies we derived a novel conclusion regarding functional crosstalk between RyRs and $InsP_3Rs$ in atrial myocytes based on highly efficient but "eventless" IP3ICR.

Identification of Ca^{2+} sparks

We analyzed individual Ca^{2+} release events triggered by photorelease of $InsP_3$. RyRs Ca^{2+} sparks are characterized by amplitudes of up to 2 $\Delta F/F_0$, widths ≈2 μm, FDHM ≈30 ms, whereas $InsP_3$ Ca^{2+} puffs are characterized by smaller amplitudes, increased widths ≈6 μm and a prolonged FDHM of about 100-600 ms (Zima & Blatter, 2004; Niggli & Shirokova, 2007; Cheng & Lederer, 2008). Our spark analysis revealed Ca^{2+} sparks but did not show a second distinct class of Ca^{2+} release events which could be *ad hoc* assigned to Ca^{2+} puffs, respectively. In addition, selective pharmacological inhibition of either $InsP_3Rs$ or RyRs let us conclude that the detected $InsP_3$ triggered Ca^{2+} release events can be classified as Ca^{2+} sparks. However, the absence of photolytically triggered IP3ICR events was surprising.

Functional crosstalk of $InsP_3R$ and RyR2 via invisible SR-Ca^{2+} release

Despite the evidence that IP3ICR occurs in cardiac cells (Zima & Blatter, 2004), reports of elementary Ca^{2+} signals arising from $InsP_3R$ openings have been rare, which may be due to the Ca^{2+} spark dominance. In atrial myocytes, $InsP_3Rs$ are colocalized with RyRs, preferentially in the subsarcolemmal space and around the nucleus (Lipp *et al*., 2000; Mackenzie *et al*., 2002). The

expression of $InsP_3Rs$ is known to be regulated in a highly dynamic manner, notably during development and cellular remodeling in pathophysiological situations (Janowski *et al*., 2006).

RyRs are arranged in functional arrays (10–300 RyRs) and subject to stochastic cluster assembly processes (Baddeley *et al*., 2009). The synchronized openings of clustered RyRs result in local Ca^{2+} sparks. Under resting conditions, in diastole, spontaneous Ca^{2+} sparks reflect the finite open probability of RyRs which is controlled by $[Ca^{2+}]_i$, luminal Ca^{2+} ($[Ca^{2+}]_{SR}$), phosphorylation state, and numerous other factors (Eisner *et al*., 1998). A comparable configuration of spatially segregated clusters of 10–100 $InsP_3Rs$ is believed to be responsible for the generation of "Ca^{2+} puffs", activated by $InsP_3$ and Ca^{2+} (Foskett *et al*., 2007), but direct ultrastructural evidence is yet missing (Shuai *et al*., 2007). In addition, there are species differences human/rat/rabbit *vs*. mouse in the $InsP_3R$ cluster dynamics and microarchitecture which shape the $InsP_3$ Ca^{2+} event characteristics (Diambra & Marchant, 2011). It has been suggested, that $InsP_3Rs$ are mobile in the SR membrane and can form clusters upon stimulation (Pantazaka & Taylor, 2011). There is also evidence that $InsP_3R$ Ca^{2+} release sites represent pre-established, stable clusters of $InsP_3Rs$ (Smith *et al*., 2009). Under this view, brief exposure to $InsP_3$ should trigger Ca^{2+} puffs, which was not the case in our study. We suggest, that $InsP_3Rs$ in intact mouse atrial myocytesmay not form sufficient cluster size to facilitate Ca^{2+} puffs due to low level of $InsP_3R$ expression and/or intercluster distance. $InsP_3Rs$ may rather be distributed near RyRs to facilitate Ca^{2+} sparks. This view is supported by our immunohistochemistry study showing that $InsP_3Rs$ seem to be rather homogeneously distributed. (see Fig. 3S, Supplementary Material). According to our data, expression of functional $InsP_3Rs$ in atrial myocytes may not necessarily lead to the formation of distinguished Ca^{2+} puffs.

Thus, how can the increase in Ca^{2+} spark frequency after $InsP_3$ photorelease be explained? The prevalent view that Ca^{2+} sparks and Ca^{2+} puffs are elementary events, becomes more comprehensive, since for both types of local Ca^{2+} release events, even smaller elementary Ca^{2+} release events have been confirmed. Compared to Ca^{2+} sparks, openings of single RyRs may result in smaller but more frequent events ("Ca^{2+} quarks") (Lipp *et al*., 1996; Brochet *et al*., 2011). At the same time, similar to Ca^{2+} quarks, $InsP_3R$-dependent elementary Ca^{2+} release events arising from single $InsP_3R$ openings, termed "Ca^{2+} blips", have been discovered (Parker *et al*., 1996). Opposed to triggered events, which are experimentally easy to detect, "blips" and "quarks" are largely invisible because these Ca^{2+} events are below detection threshold (Sobie *et al*., 2002; Williams *et al*., 2011). This is due to the low signal-to-noise ratio given by fluorescent Ca^{2+} measurements. The absence of visible Ca^{2+} puffs in our measurements, together with the observed increase in spark frequency mediated by $InsP_3Rs$, suggests a significant contribution of "invisible" or "eventless"

IP3ICR to the occurrence of Ca^{2+} sparks (and possible Ca^{2+} wave propagation). We propose that these eventless $InsP_3R$ openings may be responsible for microdomain $[Ca^{2+}]_i$ increase that either sensitize RyRs for CICR or lead to direct RyR activation. Functional crosstalk between $InsP_3R$ and RyR can operate in both directions. Hence, microdomain $[Ca^{2+}]_i$ elevations could sensitize $InsP_3R$ for $InsP_3$ which would favor $InsP_3R$ openings (Foskett *et al*., 2007).

Thus, the contribution of eventless SR-Ca^{2+} release *via* $InsP_3R$ could be more substantial for the regulation of Ca^{2+} signaling in cellular microdomains than previously thought. This is consistent with a number of not entirely explained experimental reports regarding functional interactions of $InsP_3R$ and RyR. It has been reported that $InsP_3R$ activity increases $[Ca^{2+}]_i$ in the vicinity of RyRs and thus facilitates CICR during ECC in adult cat atrial myocytes (Zima & Blatter, 2004) and that $InsP_3$-dependent Ca^{2+} release has a positive inotropic effect on ECC by facilitating Ca^{2+} release through RyR clusters in rabbit ventricle myocytes(Domeier *et al*., 2008). Furthermore, there is evidence that Ca^{2+} leak through $InsP_3Rs$ is present at sites where RyRs are located and that this Ca^{2+} leak can modulate RyR Ca^{2+} release events (Gordienko & Bolton, 2002).

This “invisible” SR-Ca^{2+} leak, respectively SR-Ca^{2+} flux *via* $InsP_3R$, was further examined in a series of SR-Ca^{2+} leak measurements. Here, $InsP_3R$ function was stimulated with ET-1. Compared to control, ET-1 may stimulate various Ca^{2+} influx pathways (e.g. via TRPC) (Treves *et al*., 2004), which may have led to an increased SR-Ca^{2+} load before the nominally Ca^{2+} and Na^+ free solution was added. This would lead *per se* to a transient increase in SR-Ca^{2+} leak until a new steady-state with matched leak/load relationship is reached. Nevertheless, increased $InsP_3R$ open probability will then concomitantly produce an “excess” SR-Ca^{2+} leak in the Ca^{2+} and Na^+ free solution compared to control as seen in Figure 4A. This is largely independent of the total SR-Ca^{2+} content and results in an increased leak/load relationship.

Taken together, experiments using photorelease of $InsP_3$ and SR-Ca^{2+} leak measurements suggest that “eventless” $InsP_3$ dependent SR-Ca^{2+} leak is the main mechanism of functional crosstalk between InsP3Rs and RyRs.

Pathophysiological implications

A change in the SR-Ca^{2+} leak/load relationship can effectively change $[Ca^{2+}]_{SR}$ transiently or even under steady-state conditions. It is well established that $[Ca^{2+}]_{SR}$ is involved in various forms of cellular instability and affected during cellular remodeling in response to pathophysiological stress (Bers, 2003; Shannon *et al*., 2003; Wehrens *et al*., 2005). Under chronic atrial fibrillation, $InsP_3Rs$ are targeted during cellular remodeling and were found to be up-regulated, which may have

positive inotropic effects on the global level (Zima & Blatter, 2004; Li *et al*., 2005; Bootman *et al*., 2007; Harzheim *et al*., 2009). Recently, subcellular mechanism(s) linking $InsP_3R$ activity to the development of atrial fibrillation and cardiac hypertrophy has been demonstrated (Higazi *et al*., 2009; Nakayama *et al*., 2010). Cardiac specific blockage of the $InsP_3R$ pathway, therefore, could offer a new therapeutic strategy for treatment of atrial arrhythmogenicity.

AUTHOR CONTRIBUTIONS

All experiments were performed at the Dept. of Physiology, University of Bern, Switzerland. M.E. conceived and designed experiments. T.H. collected and analyzed the experimental data. M.E., T.H. and N.D.U. drafted and revised the article. All authors approved the final version for publication.

ACKNOWLEDGEMENTS

We thank Ernst Niggli for valuable discussions and helpful comments on the manuscript.
This work was supported by the Swiss National Science Foundation (31-111983), Berne University Research Foundation and Novartis Res. Foundation to M.E.

FIGURE LEGEN

FIGURE 1

ET-1 induced $InsP_3R$ Ca^{2+} release in atrial myocytes

Time series of $InsP_3$ induced Ca^{2+} release events expressed as F/F_0 of fluo-3 fluorescence obtained in atrial myocytes. Cells were loaded with 5 μM fluo-3 AM (Biotium) for 20 min and left for de-estrification for 15 minutes before time series were collected in resting cells. **A.** $InsP_3$ pathway was stimulated with 100 nM ET-1 causing a substantial increase in SR-Ca^{2+} release event activity. **B.** Inhibition of ET-1-triggered Ca^{2+} events with 5 μM 2APB. **C.** Spontaneous Ca^{2+} event activity under control conditions. SR-Ca^{2+} load was measured at the end of each experiment and found not significantly different in the various conditions (CTRL: 3.45±0.28 F/F_0; ET-1: 3.89±0.48 F/F_0; 2APB+ET-1: 3.84±0.53 F/F_0). Bar graphs represent averaged F/F_0 of the first 20 s (Ctrl) and 160-200 s; scale bars represent 10 μm, N=3, n=4-9.

FIGURE 2

$InsP_3$-induced Ca^{2+} release by UV-flash photolysis of caged $InsP_3$ in atrial myocytes.

A. SR-Ca^{2+} loading protocol performed by $I_{Ca,L}$ (10 times). **B.** Representative line scan images of voltage clamped atrial myocytes in whole-cell configuration before and after UV-flash photolysis in control and with 30, 60, 240 μM caged $InsP_3$. **C.** Frequency of Ca^{2+} release events counted after UV-flash photolysis normalized to the spontaneous Ca^{2+} release events. **D.** Averaged spatio-temporal Ca^{2+} spark properties after uncaging of $InsP_3$ (240 μM) normalized to control. Cells were divided into 2 groups, white bars represent cells that showed little (<1.3) increase in Ca^{2+} release frequency (0.98±0.08 events*100$\mu m^{-1}s^{-1}$), black bars represent cells that showed >1.3 increase in Ca^{2+} release frequency (3.24±0.55 events*100$\mu m^{-1}s^{-1}$). Amplitude ($\Delta F/F_0$), full width at half-maximum amplitude (FWHM; μm), full duration at half-maximum amplitude (FDHM; ms) showed no significant difference after flash photolysis in both groups (See supplementary Table 1). Full width (μm) showed a significant increase (from 3.80±0.3 μm to 4.50±0.4 μm) in cells with low Ca^{2+} event frequency in response to photolysis. *P<0.05 vs. control, N=6-7, n=6-17, mean±SEM.

FIGURE 3

Identification of $InsP_3$ evoked Ca^{2+} sparks.

A. Experimental protocol, SR-Ca^{2+} loading protocol performed by $I_{Ca,L}$ (10 times); atrial myocytes were voltage clamped under whole-cell conditions, the pipette solution contained 240 μM caged $InsP_3$; line-scans are numbered 1-3: 1) control, 2) pharmacological interventions and 3) pharmacological interventions combined with photolytically released $InsP_3$. Modified protocols were used for the application of 2APB and TET. **B.** Representative data showing line-scan images of fluo-3 fluorescence under whole-cell conditions taken at selected time points (1) control, (2) in the presence of 2APB or TET, (3) pharmacology and photolytic release of $InsP_3$. **C.** Frequency of Ca^{2+} release events evoked by uncaging of caged $InsP_3$ normalized to control (spontaneous frequency in rest). The increase in Ca^{2+} spark frequency was inhibited by the application of either 2APB or Xesto ($InsP_3$R inhibitors) and by TET (RyR inhibitor). **D.** SR-Ca^{2+} content measured by rapid caffeine (10 mM) application. **E.** Change in background fluo-3 fluorescence F/F_0 after $InsP_3$ uncaging, in the presence of TET (dark grey) or 2APB (red). Fluorescence F/F_0 was normalized to background fluorescence before $InsP_3$ release (right). Background fluorescence increase after UV-flash photolysis of caged $InsP_3$ in the presence of TET was blocked by 2APB. *P<0.05 vs. control, N=2-5; n=6-13, mean±SEM.

FIGURE 4

Invisible $InsP_3$ dependent SR-Ca^{2+} release unmasked by SR-Ca^{2+} leak-load relationship

A. Representative data showing averaged F/F_0 of fluo-3 fluorescence changes (control: red, ET-1: black) and **B**. corresponding line-scan images of fluo-3 fluorescence recorded in atrial myocytes. Cells were field stimulated for at least 45 seconds at 1 Hz before line scan images were recorded. After pre-pulse protocol, superfusion was rapidly switched from 1.8 mM $[Ca^{2+}]_o$ to a nominally $[Ca^{2+}]_o$ and $[Na^+]_o$-free extracellular solution for 15 s, then 10 μM CPA was added for 20 s, before 10 mM caffeine was applied. The protocol was repeated in the presence of 100 nM ET-1 after pre-incubation with 100 nM ET-1 for at least 120 s. The increase in background fluorescence when CPA was applied represents SR-Ca^{2+} leak ($\Delta[Ca^{2+}]_i$). **C.** Averaged data, SR-Ca^{2+} leak ($\Delta[Ca^{2+}]_i$), SR-Ca^{2+} content and SR-Ca^{2+} leak/SR-Ca^{2+} load relationship ($\Delta[Ca^{2+}]_i$/SR-Ca^{2+} load) compared to control (no $InsP_3$ pathway stimulation). In the presence of ET-1 there was a significant increase in the SR-Ca^{2+} leak ($\Delta[Ca^{2+}]_i$) when CPA was added unmasking a substantial contribution of the $InsP_3$R opening to the total SR-Ca^{2+} leak. *P<0.02-009 vs. control, N=3; n=12-13, mean±SEM.

REFERENCES

Baddeley D, Jayasinghe ID, Lam L, Rossberger S, Cannell MB & Soeller C (2009). Optical single-channel resolution imaging of the ryanodine receptor distribution in rat cardiac myocytes. *PNAS* **106,** 22275–22280.

Bers DM (2003). Sarcoplasmic Reticulum Ca^{2+} and Heart Failure: Roles of Diastolic Leak and Ca^{2+} Transport. *Circ Res* **93,** 487–490.

Blatter LA, Kockskämper J, Sheehan KA, Zima AV, Hüser J & Lipsius SL (2003). Local calcium gradients during excitation-contraction coupling and alternans in atrial myocytes. *J Physiol* **546,** 19–31.

Bootman MD, Harzheim D, Smyrnias I, Conway SJ & Roderick HL (2007). Temporal changes in atrial EC-coupling during prolonged stimulation with endothelin-1. *Cell Calcium* **42,** 489–501.

Brochet DXP, Xie W, Yang D, Cheng H & Lederer WJ (2011). Quarky calcium release in the heart. *Circ Res* **108,** 210–218.

Cheng H & Lederer WJ (2008). Calcium sparks. *Physiol Rev* **88,** 1491–1545.

Cheng H, Lederer WJ & Cannell MB (1993). Calcium sparks: elementary events underlying excitation-contraction coupling in heart muscle. *Science* **262,** 740–744.

Domeier TL, Zima AV, Maxwell JT, Huke S, Mignery GA & Blatter LA (2008). IP_3 receptor-dependent Ca^{2+} release modulates excitation-contraction coupling in rabbit ventricular myocytes. *Am J Physiol* **294,** H596–H604.

Eisner DA, Trafford AW, Diaz ME, Overend CL & O'Neill SC (1998). The control of Ca^{2+} release from the cardiac sarcoplasmic reticulum: regulation versus autoregulation. *Cardiovasc Res* **38,** 589–604.

Foskett JK, White C, Cheung K-H & Mak D-OD (2007). Inositol trisphosphate receptor Ca^{2+} release channels. *Physiol Rev* **87,** 593–658.

Gordienko D & Bolton T (2002). Crosstalk between ryanodine receptors and IP_3 receptors as a factor shaping spontaneous Ca^{2+}-release events in rabbit portal vein myocytes. *J Physiol* **542,** 743–762.

Harzheim D, Movassagh M, Foo RS-Y, Ritter O, Tashfeen A, Conway SJ, Bootman MD & Roderick HL (2009). Increased $InsP_3Rs$ in the junctional sarcoplasmic reticulum augment Ca^{2+} transients and arrhythmias associated with cardiac hypertrophy. *PNAS* **106,** 11406–11411.

He JQ, Pi Y, Walker JW & Kamp TJ (2000). Endothelin-1 and photoreleased diacylglycerol increase L-type Ca^{2+} current by activation of protein kinase C in rat ventricular myocytes. *J Physiol* **3,** 807–820.

Higazi DR, Fearnley CJ, Drawnel FM, Talasila A, Corps EM, Ritter O, McDonald F, Mikoshiba K, Bootman MD & Roderick HL (2009). Endothelin-1-stimulated $InsP_3$-induced Ca^{2+} release is a nexus for hypertrophic signaling in cardiac myocytes. *Mol Cell* **33,** 472–482.

Janowski E, Cleemann L, Sasse P & Morad M (2006). Diversity of Ca^{2+} signaling in developing cardiac cells. *Ann NY Acad Sci* **1080,** 154–164.

Kockskämper J, Zima AV, Roderick HL, Pieske B, Blatter LA & Bootman MD (2008). Emerging roles of inositol 1,4,5-trisphosphate signaling in cardiac myocytes. *J Mol Cell Cardiol* **45,** 128–147.

Li X, Zima AV, Sheikh F, Blatter LA & Chen J (2005). Endothelin-1-induced arrhythmogenic Ca^{2+} signaling is abolished in atrial myocytes of inositol-1,4,5-trisphosphate(IP_3)-receptor type 2-deficient mice. *Circ Res* **96,** 1274–1281.

Lipp P, Laine M, Tovey SC, Burrell KM, Berridge MJ, Li W & Bootman MD (2000). Functional $InsP_3$ receptors that may modulate excitation-contraction coupling in the heart. *Curr Biol* **10,** 939–942.

Lipp P, Lüscher C & Niggli E (1996). Photolysis of caged compounds characterized by ratiometric confocal microscopy: a new approach to homogeneously control and measure the calcium concentration in cardiac myocytes. *Cell Calcium* **19,** 255–266.

Mackenzie L, Bootman M, Laine M, Berridge M, Thuring J, Holmes A, Li W & Lipp P (2002). The role of inositol 1,4,5-trisphosphate receptors in Ca^{2+} signalling and the generation of arrhythmias in rat atrial myocytes. *J Physiol* **541,** 395–409.

Mackenzie L, Roderick HL, Berridge MJ, Conway SJ & Bootman MD (2004). The spatial pattern of atrial cardiomyocyte calcium signalling modulates contraction. *J Cell Sci* **117,** 6327–6337.

Nakayama H, Bodi I, Maillet M, DeSantiago J, Domeier T, Mikoshiba K, Lorenz J, Blatter L, Bers D & Molkentin J (2010). The IP_3 receptor regulates cardiac hypertrophy in response to select stimuli. *Circ Res* **107,** 659–666.

Niggli E & Shirokova N (2007). A guide to sparkology: the taxonomy of elementary cellular Ca^{2+} signaling events. *Cell Calcium* **42,** 379–387.

Pantazaka E & Taylor CW (2011). Differential distribution, clustering, and lateral diffusion of subtypes of the inositol 1,4,5-trisphosphate receptor. *J Biol Chem* **286,** 23378–23387.

Parker I, Choi J & Yao Y (1996). Elementary events of $InsP_3$-induced Ca^{2+} liberation in Xenopus oocytes: hot spots, puffs and blips. *Cell Calcium* **20,** 105–121.

Picht E, Zima AV, Blatter LA & Bers DM (2007). SparkMaster: automated calcium spark analysis with ImageJ. *Am J Physiol* **293,** C1073–C1081.

Shannon TR, Ginsburg KS & Bers DM (2002). Quantitative assessment of the SR Ca^{2+} leak-load relationship. *Circ Res* **91,** 594–600.

Shannon TR, Pogwizd SM & Bers DM (2003). Elevated sarcoplasmic reticulum Ca^{2+} leak in intact ventricular myocytes from rabbits in heart failure. *Circ Res* **93,** 592–594.

Shuai J, Pearson JE, Foskett JK, Mak D-OD & Parker I (2007). A kinetic model of single and clustered IP_3 receptors in the absence of Ca^{2+} feedback. *Biophys J* **93,** 1151–1162.

Smith IF, Wiltgen SM, Shuai J & Parker I (2009). Ca^{2+} puffs originate from preestablished stable clusters of inositol trisphosphate receptors. *Sci Signaling* **2,** 1-7.

Sobie E, Dilly K, Cruz J, Lederer J & Jafri M (2002). Termination of cardiac Ca^{2+} sparks: An investigative mathematical model of calcium-induced calcium release. *Biophys J* **83,** 59–78.

Treves S, Franzini-Armstrong C, Moccagatta L, Arnoult C, Grasso C, Schrum A, Ducreux S, Zhu MX, Mikoshiba K & Girard T (2004). Junctate is a key element in calcium entry induced by activation of $InsP_3$ receptors and/or calcium store depletion. *J Cell Biol* **166,** 537–548.

Wehrens XHT, Lehnart SE & Marks AR (2005). Intracellular Calcium Release and Cardiac Disease. *Annu Rev Physiol* **67,** 69–98.

Williams GSB, Chikando AC, Tuan H-TM, Sobie EA, Lederer WJ & Jafri MS (2011). Dynamics of calcium sparks and calcium leak in the heart. *Biophys J* **101,** 1287–1296.

Yamasaki Y, Furuya Y, Araki K, Matsuura K, Kobayashi M & Ogata T (1997). Ultra-high-resolution scanning electron microscopy of the sarcoplasmic reticulum of the rat atrial myocardial cells. *Anat Rec* **248,** 70–75.

Yao Y, Choi J & Parker I (1995). Quantal puffs of intracellular Ca^{2+} evoked by inositol trisphosphate in Xenopus oocytes. *J Physiol* **482,** 533–553.

Zima AV & Blatter LA (2004). Inositol-1,4,5-trisphosphate-dependent Ca^{2+} signalling in cat atrial excitation-contraction coupling and arrhythmias. *J Physiol* **555,** 607–615.

ONLINE SUPPLEMENTS

Material and Methods

Atrial myocytes from adult male C57/BL6 mice, obtained from the Central Animal Facility, University Hospital, University of Bern, were freshly isolated by Langendorff perfusion technique. All experiments were approved by the State Veterinary Office of Bern, Switzerland, according to Swiss Federal Animal protection law. The authors have also read, and the experiments comply with, the policies and regulations of *The Journal of Physiology* described by Drummond, 2009 (Drummond, 2009). Adult male C57/BL6 mice (3-5 months old) were heparinized (50 U ip) and subsequently killed after 5-15 minutes by cervical dislocation. Hearts were rapidly removed and mounted on a Langendorff column and perfused retrogradely for 8-16 minutes with collagenase type II (14 U/ml, Worthington type 2) and protease type IV (0.2 U/ml, Sigma, type XIV) in a Ca^{2+} free solution (in mmol/L: 140 NaCl, 5.4 KCl, 1.1 $MgCl_2$, 1 Na_2HPO_4, 5 HEPES and 10 glucose at pH 7.4, 37ºC). Atria (auricle) were removed and rinsed in 1% BSA solution before cells were dissociated mechanically from the tissue in Ca^{2+} free solution. The free $[Ca^{2+}]_o$ was increased progressively to 500-700 μM over 1-2 hours before cells were used for experiments within 4 hours after isolation. All experiments were performed at room temperature.

HeLa cells were a kind gift from N. Demaurex's lab, Geneva. HeLa cells were cultured on glass cover slips in DMEM, 10% FBS, 1% HEPES, 0.1% penicillin / streptomycin until 80% confluent. Once 80% confluency was reached, cells were used for experiments. Ca^{2+} responses were detected with K_5-fluo-3 after flash photolysis of 30 μM caged $InsP_3$ in the patch pipette.

Patch Clamp Recordings with caged $InsP_3$. Electrophysiological recordings were combined with simultaneous confocal Ca^{2+} imaging. Caged $InsP_3$ (Sichem) was dialyzed into the atrial myocytes via low resistance pipettes (1.5-3 MΩ) which were pulled from borosilicate glass micropipettes using a Zeitz DMZ puller (Zeitz instruments, Germany). The pipette solution contained (in mmol/L) 120 CsAsp, 10 HEPES, 20 TEA-Cl, 5 K-ATP,1 $MgCl_2$, 0.1 K_5-fluo-3 (Biotium), 2 GSH, (0.03, 0.06, 0.24) caged $InsP_3$ 6Na (Sichem), pH 7.2 with CsOH. Free Ca^{2+} was calculated using Patcher's Power Tools (IgorPro plug-in, MPI Göttingen, Germany) and was approximately 59 nM. During the experimental procedure, cells were perfused with external solution containing (in mmol/L) 140 NaCl, 5 HEPES, 1.1 $MgCl_2$, 5.4 KCl, 10 Glucose, 1.8 $CaCl_2$, 0.5 BaCl, 1 CsCl, pH 7.4 NaOH. Pharmacological experiments used 5 μM 2-aminoethoxydiphenyl borate (2APB, Fluka), 5 μM xestospongin C (Xesto, A.G Scientific Inc), 1 mM tetracaine (TET, Sigma) or 10 mM caffeine (Sigma) added to the external solution.

Figure 1

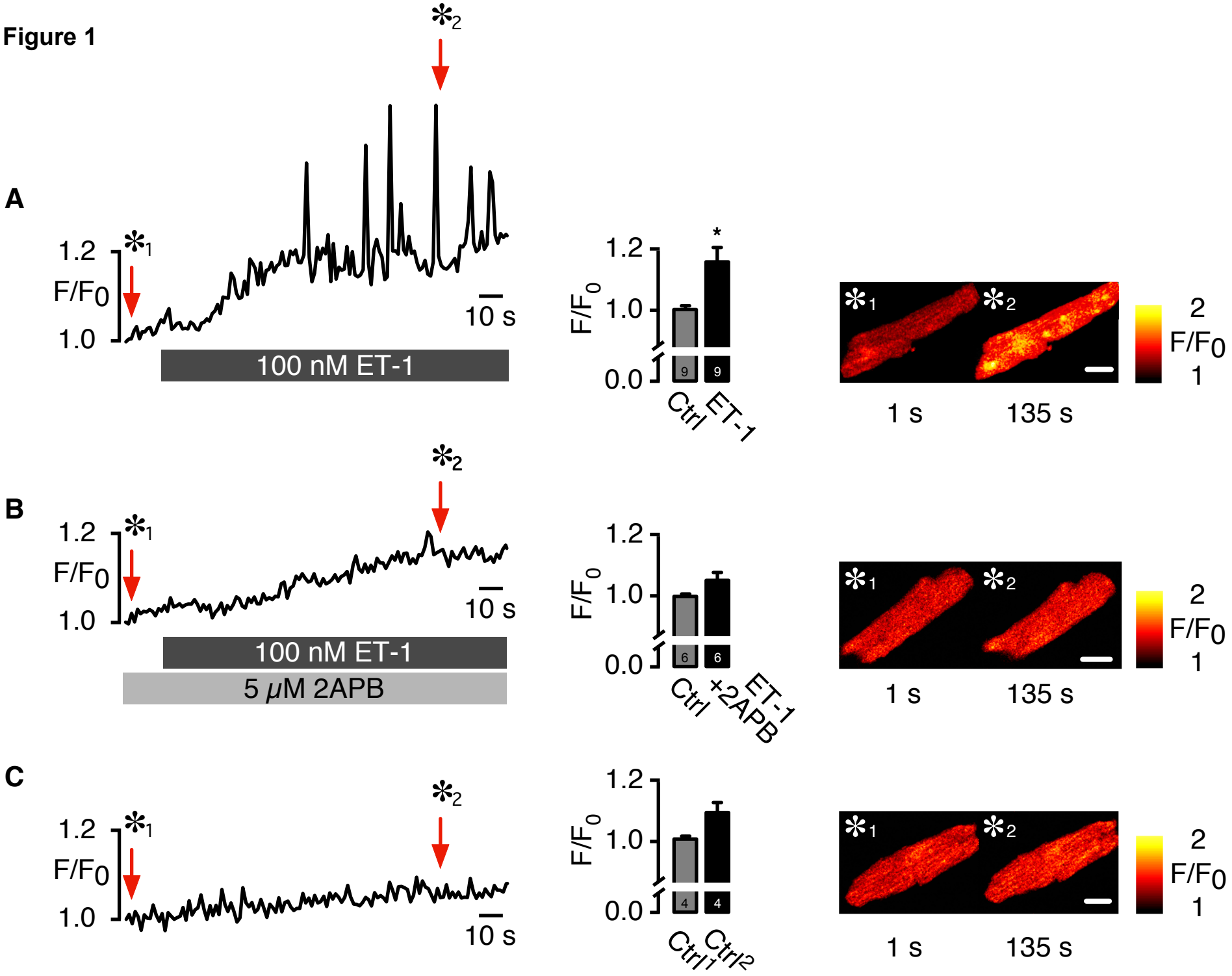
A
B
C
1.2
F/F0
1.0
10 s
100 nM ET-1
5 μM 2APB
0.0
Ctrl
ET-1
ET-1 +2APB
Ctrl1
Ctrl2
1 s
135 s
2
1

Figure 2

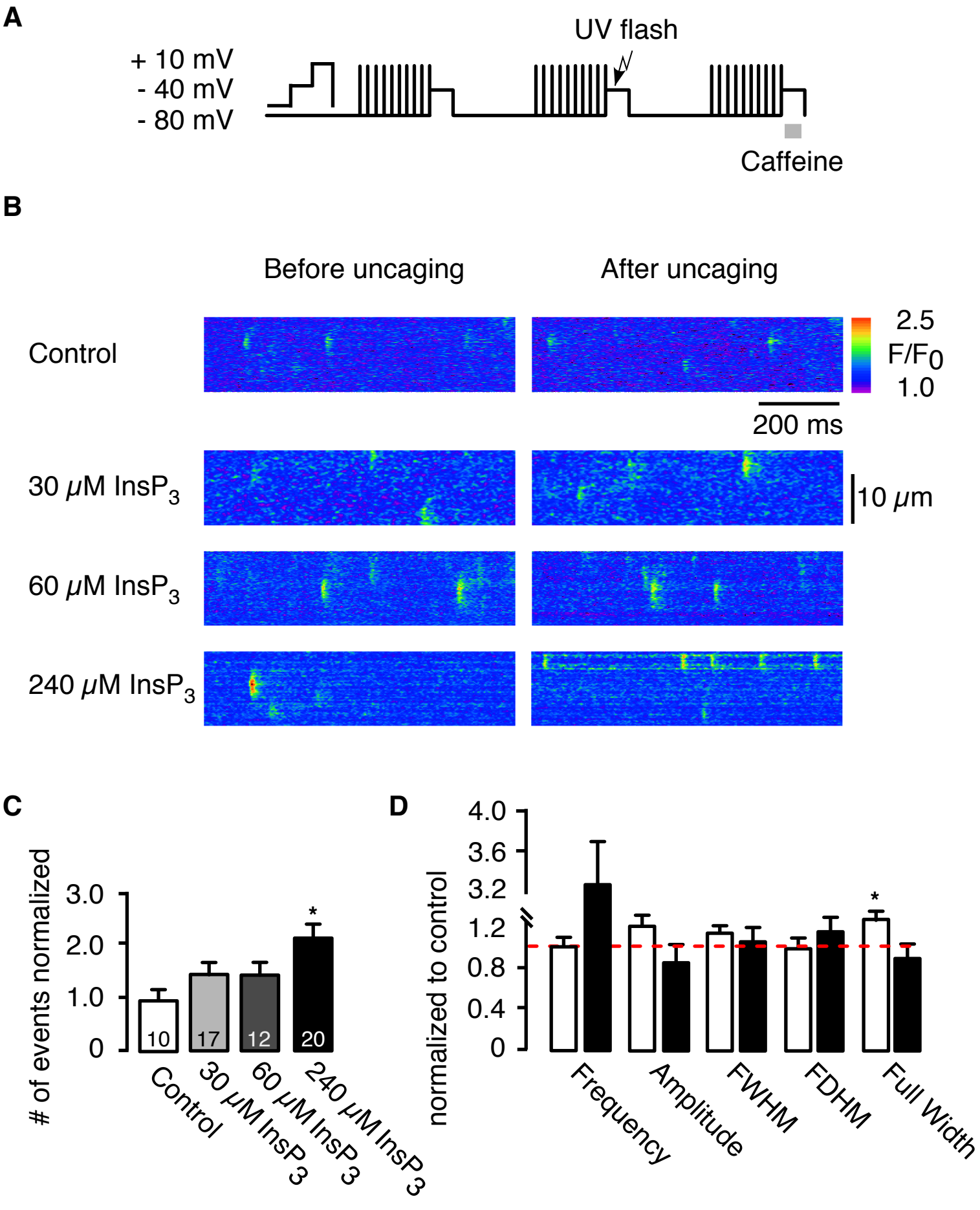
A
UV flash
+ 10 mV
- 40 mV
- 80 mV
Caffeine
B
Before uncaging
After uncaging
Control
2.5
F/F0
1.0
200 ms
30 μM InsP3
10 μm
60 μM InsP3
240 μM InsP3
C
# of events normalized
3.0
2.0
1.0
0
10
17
12
20
*
Control
30 μM InsP3
60 μM InsP3
240 μM InsP3
D
normalized to control
4.0
3.6
3.2
1.2
0.8
0.4
0
*
Frequency
Amplitude
FWHM
FDHM
Full Width

Figure 3

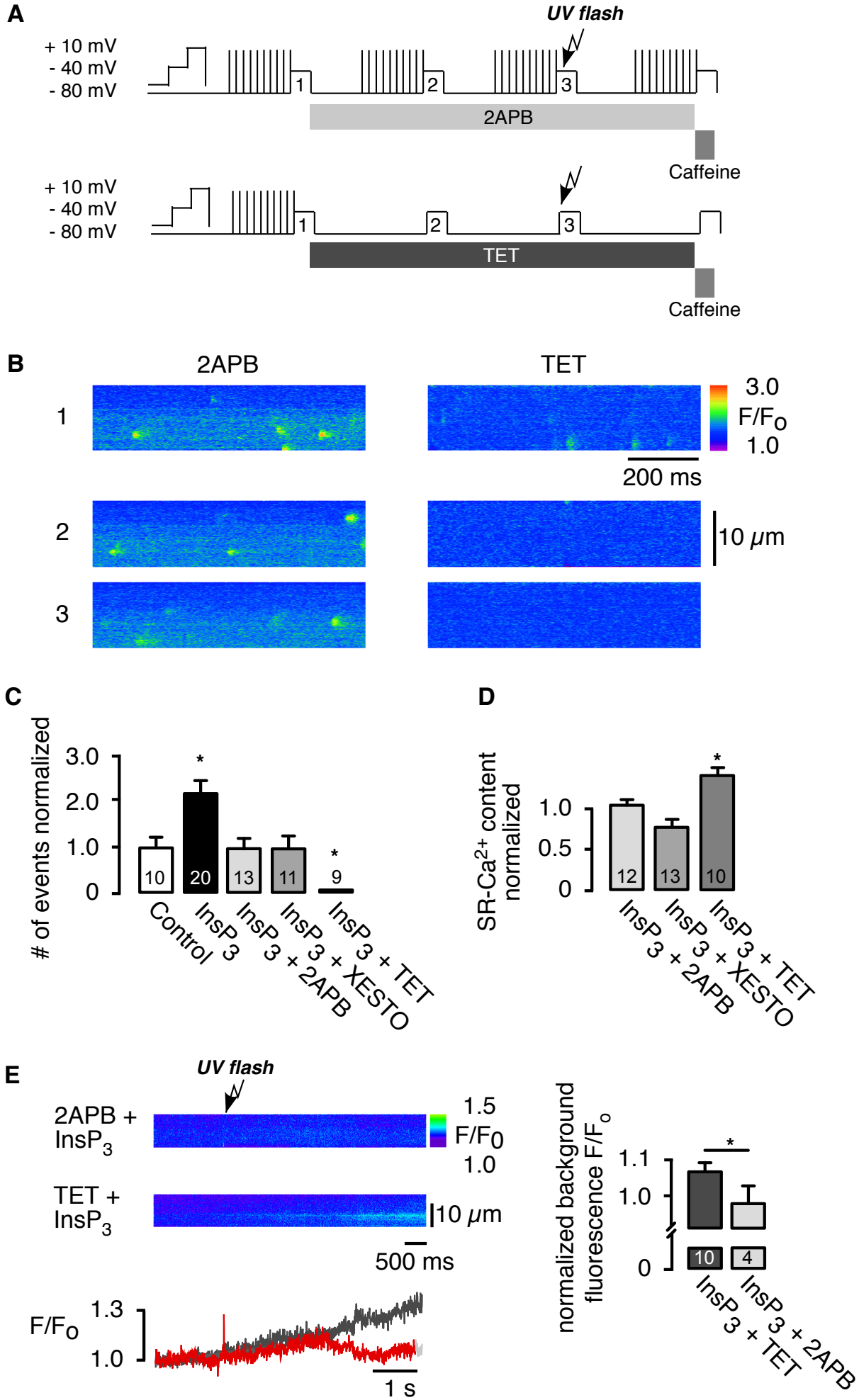
A
UV flash
+ 10 mV
- 40 mV
- 80 mV
1
2
3
2APB
Caffeine
TET
B
2APB
TET
3.0
F/Fo
1.0
200 ms
10 μm
C
# of events normalized
Control
InsP3
InsP3 + 2APB
InsP3 + XESTO
InsP3 + TET
D
SR-Ca2+ content normalized
E
2APB + InsP3
TET + InsP3
1.5
F/F0
500 ms
1.3
1 s
normalized background fluorescence F/Fo
1.1

Figure 4

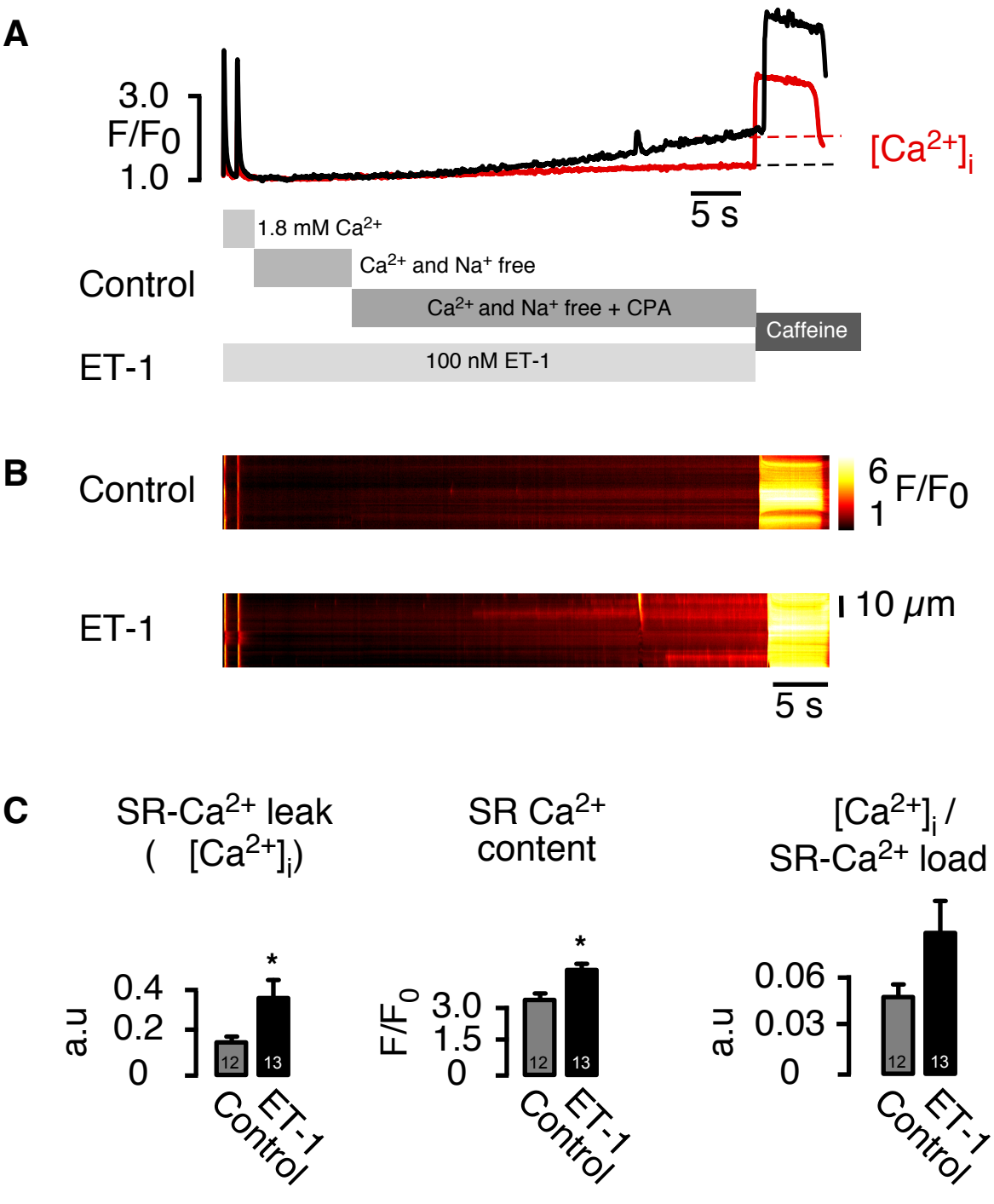
A
3.0
F/F0
1.0
[Ca2+]i
5 s
1.8 mM Ca2+
Ca2+ and Na+ free
Control
Ca2+ and Na+ free + CPA
Caffeine
ET-1
100 nM ET-1
B
Control
6
1
F/F0
ET-1
10 μm
5 s
C
SR-Ca2+ leak
([Ca2+]i)
SR Ca2+
content
[Ca2+]i /
SR-Ca2+ load
a.u
0.4
0.2
0
F/F0
3.0
1.5
0
0.06
0.03
0
12
13
Control
ET-1
*

Cells were held at -80 mV and depolarized from -80 mV to 0mV ten times before line-scan images were taken; membrane voltages were controlled with an Axopatch 200 amplifier (Axon Instruments, Foster City, CA) driven by custom-written software developed under LabView software (National Instruments). Fluo-3 was excited with the 488 nm line of an argon laser alternatively with a solid-state laser (50 μW; Sapphire, Coherent) and fluorescence (> 515 nm) in line-scan mode (6 ms/line) was collected with a PMT on an MRC-100 or MicroRadiance confocal microscope (both BioRad, Glattbrugg, Switzerland). Line-scans of 1024 lines were collected in 2 equal, sequential segments. In line-scan recordings where $InsP_3$ was uncaged, UV light from a xenon short-arc flash lamp (300-350 nm, pulse duration ~ 400 μs, discharge energy up to 230 J) was delivered and applied at the beginning of line-scan recordings. For more details see Del Principe *et al*. (DelPrincipe *et al*., 1999). Line-scan images were processed using customized Image SXM software (Steve Barrett, University of Liverpool, UK). 3000 ms were used for analysis of each line-scan. Sparkmaster plug-in (Picht *et al*., 2007) for ImageJ (Wayne Rassband, NIH, USA) was used to identify and analyze Ca^{2+} release events. IgorPRO (WaveMatrics, Portland, OR, USA) software was used to analyze caffeine transients.

Ca^{2+} leak measurements. Using the RyR2 blocker TET, Ca^{2+} leak was determined and using the SR-Ca^{2+} pump (SERCA) blocker cyclopiazonic acid (CPA), the increase in $[Ca^{2+}]_i$ ($\Delta[Ca^{2+}]_i$) was determined with an adapted protocol from Shannon *et al*. (Shannon *et al*., 2002). Line-scans were recorded at 50 l/s on a laser scanning confocal microscope (MicroRadiance, BioRad, UK). Atrial myocytes were loaded with 5 μM fluo-3 AM (Biotium) for 20 min and left for de-estrification for 15 minutes before confocal images were collected. Fluo-3 (Biotium) was excited using an argon ion laser. Cells were field stimulated for at least 45 seconds at 1 Hz before line-scan images were recorded. After the pre-loading protocol, superfusion was rapidly switched from (in mmol/L) 140 NaCl, 5 KCl, 5 HEPES, 1 MgCl, 1.8 $CaCl_2$, 10 glucose, pH 7.4 with NaOH to a nominally Na^+ and Ca^{2+}-free solution (by substitution of Na^+ with Li^+ and addition of 0.5 mmol/L EGTA). A further solution switch was done after 10 s to a nominally Ca^{2+} and Na^+ free solution containing CPA for 30 s, before caffeine was applied to measure SR-Ca^{2+} load. The same protocol was repeated in the presence of 100 nM ET-1 in all solutions. CPA application was accompanied with an increase in $[Ca^{2+}]_i$.

Immunofluorescent staining. Atrial myocytes were enzymatically isolated as described earlier. Without increasing Ca^{2+}, 500 μl cell dispersion was left to settle for 2 hours at room temperature on previously prepared gelatin coated coverslips. Samples were washed twice before they were fixed in 4 % paraformaldehyde for 10 minutes. Prior to staining, samples were washed one more time with

PBS before cells were permeabilized and unspecific sites were blocked for 30 min in 0.1% Triton-X-100, 5 % BSA in PBS. Myocytes were stained against InsP3R2 and RyRs by incubating the samples with rabbit polyclonal $InsP_3R2$ (Abcam, 1:500, Cat.# ab77838, see also Wang *et al.,* 2012) and mouse monoclonal RyR (Abcam 1:200, Cat.# ab2827) antibodies overnight at 4ºC in 0.1% Triton-X-100, 5 % BSA in PBS. Cells were then again washed 3 times in 0.1% Triton-X-100, 5 % BSA in PBS for 10 minutes before incubating with the secondary antibodies (Alexa Fluo 488, 1:1000; Alexa Fluo 568, 1:1000) and DAPI , 1:20000 for 1.5 hours at room temperature. Cells were then washed 3 times with PBS before coverslips were mounted on slides with mounting medium (Fluoroshield). Cells were imaged using a fluorescent microscope (TMD300 microscope, Nikon) equipped with a high-sensitivity Visicam camera (Visitron Systems, Germany).

Verification of $InsP_3R$ Ca^{2+} release

In a series of control experiments we ruled out flaws in the applied experimental settings. HeLa cells are known to have a highly developed $InsP_3R$ pathway and were used as a bio-indicator for $InsP_3$ Ca^{2+} response. HeLa cells have several advantages, they express $InsP_3R$ at high density and $InsP_3R$ dependent elementary Ca^{2+} release events are well characterized. Although they express mainly type 1 and type 3 isoforms, $InsP_3Rs$ type 2 are also present (Tovey *et al*., 2001). This workaround was inevitable because there is still a deficit in the availability of $InsP_3$ indicators which could be used to monitor rapid intracellular $InsP_3$ -mediated signals. Indeed, by using UV-flash photolysis, robust $InsP_3$ Ca^{2+} transients were elicited (Fig. 1S). As shown in Fig. 1S, using identical settings and solutions containing 30 μM caged $InsP_3$, reliable global Ca^{2+} transients were photolytically triggered. This suggests that UV-flash triggered IP3ICR can be obtained similarly in cardiac cell preparations. The reliability of the experimental approach was further underscored by the dose dependency of $InsP_3$-induced increase in Ca^{2+} event frequency (Fig. 2C).

As a positive control for elementary Ca^{2+} release events we used neonatal rat cardiomyocytes that are known to exhibit both Ca^{2+} puffs and Ca^{2+} sparks (Luo *et al*., 2008). Fig. 2S A,B and C show individual photolytically triggered $InsP_3$ "Ca^{2+} puffs", "Ca^{2+} sparks" and local mini-waves identified by their spatio-temporal properties (Niggli & Shirokova, 2007).

For a variety of caged compounds it is known that only a small fraction of the total amount of the compound is being uncaged during a single UV-flash. This essentially depends on the physicochemical properties of the compound (e.g. quantum yield), the power of UV-light and the duration of illumination (Ellis-Davies, 2007), which in our hands is in the range of 200 μs. In addition, the pipette solution contains an infinite reservoir for caged $InsP_3$ compared to the cell volume. Finally, we would expect to end up in a biologically relevant concentration range of approximatively 10 nM - 1 μM $InsP_3$.

Figure 1S

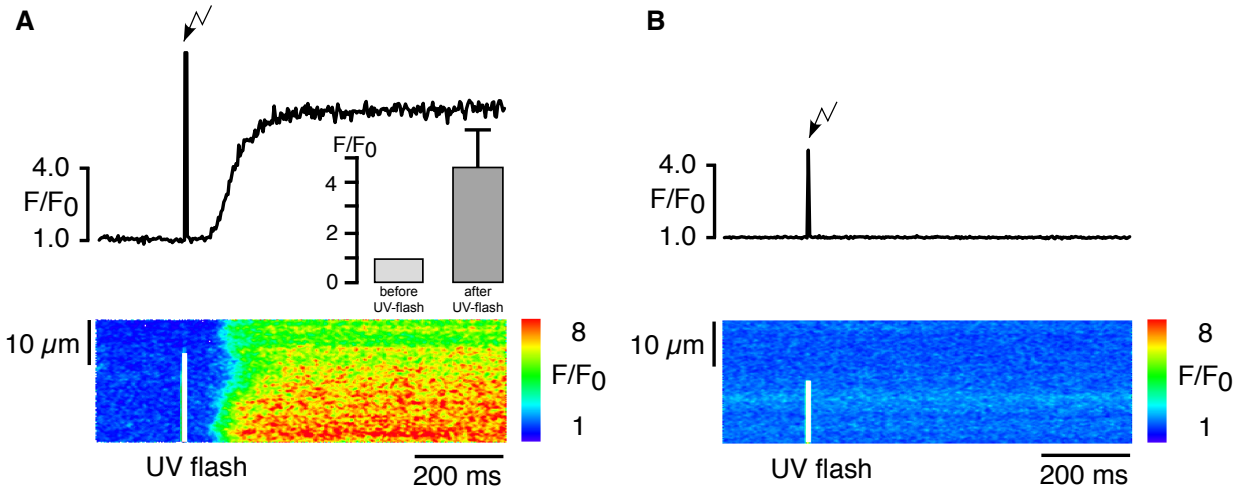

Experimental approach to verify intracellular $InsP_3$ release.

Representative data showing averaged F/F_0 of fluo-3 and corresponding line-scan images of changes in $[Ca^{2+}]_i$ in HeLa cells under whole-cell conditions of the patch-clamp technique. $InsP_3$ was released by UV-flash photolysis. **A**. With 30 μM caged $InsP_3$ in the patch pipette there is an immediate global increase in Ca^{2+} after UV flash photolysis observed in 100% of all approached cells. The inset shows normalized fluorescence F/F_o before and after UV-flash (n=6); **B**. Control, with no $InsP_3$ in the patch pipette, shows no response to flash photolysis. n=5-12

Figure 2S

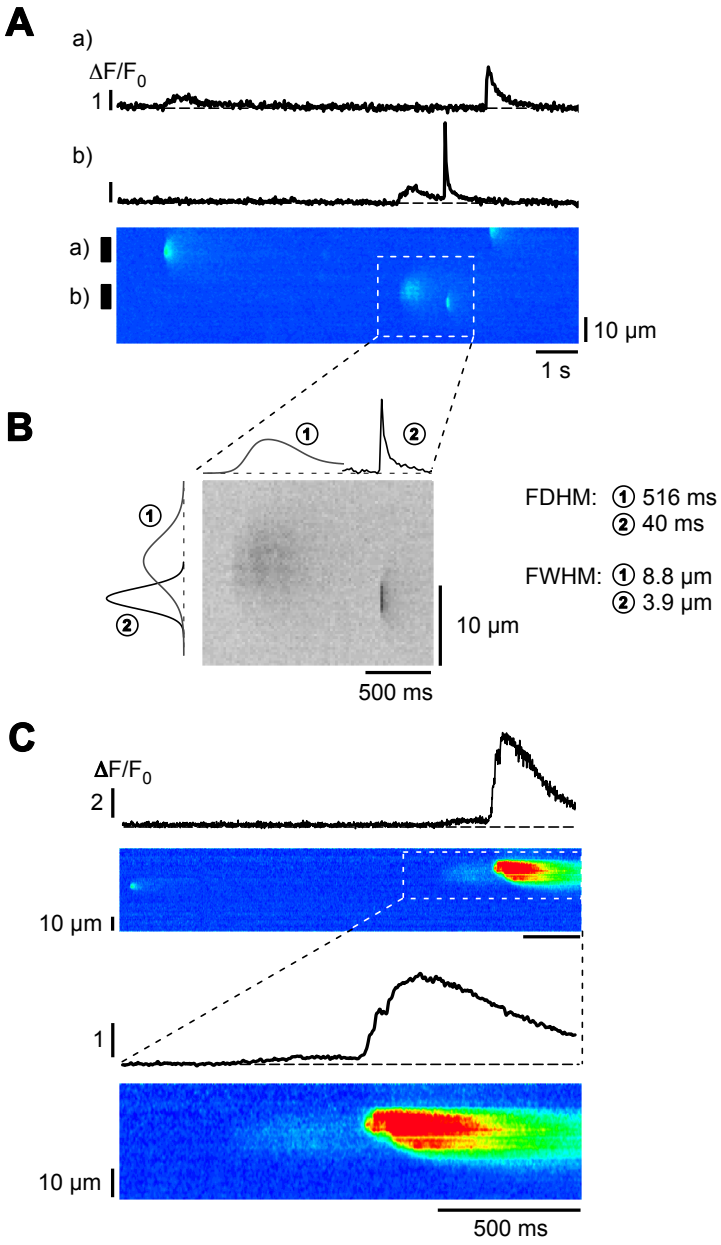

Figure 2S. Representative data showing averaged $\Delta F/F_0$ of fluo-3 fluorescence and corresponding line-scan images of changes in $[Ca^{2+}]_i$ in neonatal rat myocytes in response to $InsP_3$ photorelease. Cells were loaded with 5 μM $InsP_3$-PM (D-2,3-O-Isopropylidene-6-O-(2-Nitro-4,5-Dimethoxy) benzyl-myo-Inositol-1,4,5-Trisphosphate-Hexakis Propionoxymethyl Ester, SiChem) together with 4 μM fluo-3-AM (Biotium) for 120 and 30 min at room temperature, respectively. $InsP_3$ was liberated by UV-flash photolysis as described in the Material and Methods section. **A. a), b)** Individually triggered Ca^{2+} puff consecutively followed by a Ca^{2+} spark. **B.** Expanded part of the line-scan given above, now presented in unprocessed raw data format. From FDHM and FWHM analysis (1) can be classified as Ca^{2+} puff and (2) as Ca^{2+} spark (Picht *et al.*, 2007). **C.** Ca^{2+} mini-wave elicited in response of initial $InsP_3$ triggered local $[Ca^{2+}]_i$ increase. This local Ca^{2+} response shows that elementary Ca^{2+} release *via* $InsP_3R$ may be involved in the conditioning of CICR (e.g. Ca^{2+} mini-waves as given in this example) in cardiac cells.

Figure 3S

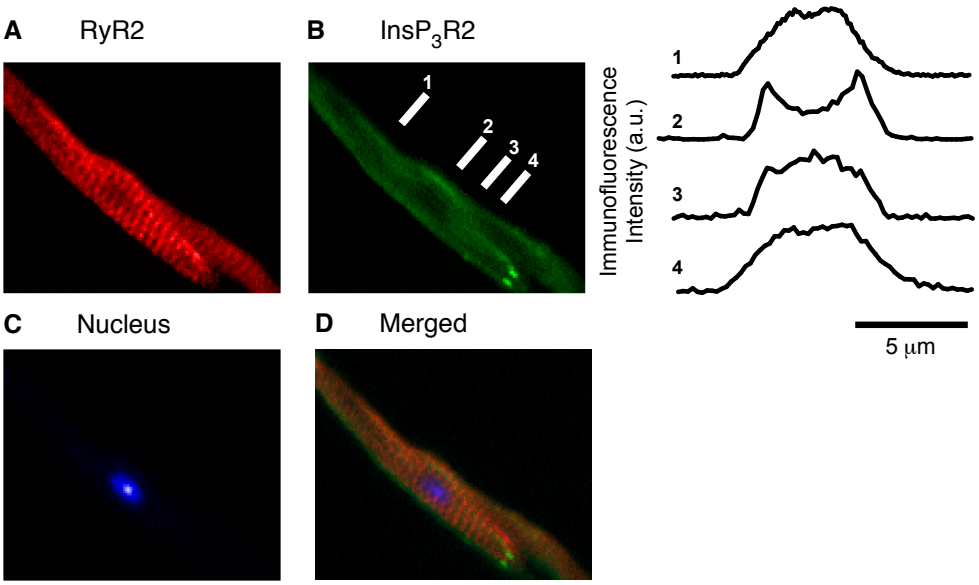

Figure 3S. Colocalization of RyR2 and $InsP_3R2$ in an atrial myocyte. **A**. Atrial myocyte was stained against RyR2 (primary antibody from Abcam 1:200, secondary Alexa Fluo 568 1:1000) **B**. Atrial myocyte was stained against $InsP_3R2$ (primary antibody from Abcam 1:500, secondary Alexa Fluo 488 1:1000), intensity profiles of immunofluorescence across the cell (right). These profiles were obtained by sampling the immunofluorescence intensity of the $InsP_3R2$ isoform across a line one pixel wide. **C**. The nucleus of atrial myocyte was stained with DAPI 1:20000 **D**. Merged image.

Ca^{2+} Spark characteristics.

Ca^{2+} spark characteristics were analyzed as mentioned in the Material and Methods section. Myocytes were divided into two groups.

Supplementary Table 1

events*100μm^{-1}s^{-1} <1.3 *10 myocytes, 4 animals*	**No $InsP_3$**	**$InsP_3$**	**p value**
Ampl ($\Delta F/F_0$)	0.79±0.05	0.87±0.06	0.33
FWHM (μm)	2.71±0.17	2.98±0.27	0.23
FDHM (ms)	51.6±2.6	50.03±3.18	0.67
fullwidth (μm)	**3.80±0.29**	**4.51±0.38**	**0.02**
fulldur (ms)	93.52±5.96	107.49±6.43	0.07
rise time (ms)	32.79±3.09	35.75±4.53	0.06
events*100μm^{-1}s^{-1} >1.3 *9 myocytes 5 animals*	**No $InsP_3$**	**$InsP_3$**	**p value**
Ampl ($\Delta F/F_0$)	1.11±0.05	0.83±0.06	0.19
FWHM (μm)	2.84±0.18	2.60±0.28	0.47
FDHM (ms)	47.87±2.75	47.62±3.35	0.97
fullwidth (μm	4.82±0.30	4.11±0.40	0.24
fulldur (ms)	120±6.28	99.74±6.78	0.31
rise time (ms)	50.60±3.25	36.88±4.77	0.18

REFERENCES

DelPrincipe F, Egger M & Niggli E (1999). Calcium signalling in cardiac muscle: refractoriness revealed by coherent activation. *Nat Cell Biol* **1,** 323–329.

Drummond GB (2009). Reporting ethical matters in the Journal of Physiology: standards and advice. *J Physiol* **587,** 713–719.

Ellis-Davies GCR (2007). Caged compounds: photorelease technology for control of cellular chemistry and physiology. *Nat Meth* **4,** 619–628.

Luo D, Yang D, Lan X, Li K, Li X, Chen J, Zhang Y, XIAO R-P, Han Q & Cheng H (2008). Nuclear Ca^{2+} sparks and waves mediated by inositol 1,4,5-trisphosphate receptors in neonatal rat cardiomyocytes. *Cell Calcium* **43,** 165–174.

Niggli E & Shirokova N (2007). A guide to sparkology: the taxonomy of elementary cellular Ca^{2+} signaling events. *Cell Calcium* **42,** 379–387.

Picht E, Zima AV, Blatter LA & Bers DM (2007). SparkMaster: automated calcium spark analysis with ImageJ. *Am J Physiol* **293,** C1073–C1081.

Shannon TR, Ginsburg KS & Bers DM (2002). Quantitative assessment of the SR Ca^{2+} leak-load relationship. *Circ Res* **91,** 594–600.

Tovey SC, De Smet P, Lipp P, Thomas D, Young KW, Missiaen L, De Smedt H, Parys JB, Berridge MJ, Thuring J, Holmes A & Bootman MD (2001). Calcium puffs are generic $InsP_3$-activated elementary calcium signals and are downregulated by prolonged hormonal stimulation to inhibit cellular calcium responses. *J Cell Sci* **114,** 3979–3989.

Wang Y, Li G, Goode J, Paz JC, Ouyang K, Screaton R, Fischer WH, Chen J, Tabas I & Montminy M (2012). Inositol-1,4,5-trisphosphate receptor regulates hepatic gluconeogenesis in fasting and diabetes. *Nature* **485,** 128–132.